J|A|C|S ARTICLES

Published on Web 06/30/2010

Cutting of Oxidized Graphene into Nanosized Pieces

Shintaro Fujii* and Toshiaki Enoki

Department of Chemistry, Tokyo Institute of Technology, 2-12-1 Ookayama, Meguro-ku, Tokyo 152-8551, Japan

Received February 11, 2010; E-mail: fujii.s.af@m.titech.ac.jp

Abstract: We report a simple approach to producing nanosized graphene on the basis of chemical oxidation of a graphene sheet followed by cutting of the sheet using a scanning probe microscopic (SPM) manipulation technique. The structural and electronic properties of the oxidized sheet are characterized by noncontact atomic force microscopic (NC-AFM) imaging and SPM spectroscopy under ultrahigh vacuum conditions. Regularly spaced linear defects with a spacing of 5−10 nm and a length of >100 nm were found on the sheet, which can be attributed to the result of linear arrangement of epoxide functional groups. The cutting experiments are performed on sheets in which the linear defects were observed in advance. Cutting is initiated by a point contact between the preoxidized sheet and the AFM probe. The local mechanical stress caused by the point contact leads to rupture of the sheet, which proceeds linearly along the linear defect of the epoxide groups. We propose that the linear defect structures can be used as a template to determine the cutting direction of the sheet. According to recently proposed theoretical predictions, the linear epoxide groups have preferential alignment along a zigzag direction in the graphene lattice, and therefore, the cut edge shape could have well-defined alignment along the zigzag direction. This cutting procedure of the graphene sheet could be a useful method for the production of nanosized graphene with well-defined edges.

1. Introduction

Graphene, a two-dimensional honeycomb lattice of sp^2-carbon atoms, has attracted intensive research interest mostly due to its unique electronic properties, such as extremely high carrier mobility[1] and anomalous quantum Hall effect,[2] which are a consequence of massless Dirac fermions with linear energy dispersion in the electronic band structure.[3] Beside these intrinsic electronic properties of graphene, it has been theoretically predicted[4,5] and substantially confirmed by scanning tunneling microscopic observations[6,7] that the finite size effect of graphene on the nanometer scale is critical in the electronic structures. There are two types of graphene edges, armchair and zigzag, and the electronic structure of nanosized graphene (nanographene) is strongly dependent on the edge geometry; the nonbonding π-electron state (edge state) is present in the zigzag edge but absent in the armchair edge. For example, zigzag graphene nanoribbon, a strip of narrow one-dimensional graphene sheet terminated by zigzag edges on both sides, has been suggested to have a peculiar localized edge state, and the localized spins of the edge state give rise to unique magnetic properties.[4,5] Similarly, very recent theoretical studies have shown that nanosized graphene with zigzag edges having different shapes, such as triangular and hexagonal islands, should also have unique magnetic properties.[8,9] The applications of the finite size effect require proper nanofabrication for tailoring of the graphene sheets into desired geometries with specific size.[10−18] Previous attempts to cut graphene have involved (i) a combination of electron beam lithography and plasma etching of graphene,[11,12] (ii) chemical stripping of graphite to obtain graphene ribbons,[13] (iii) electrochemical etching of graphite based on scanning tunneling microscopy,[14] (iv) catalytic reaction of Fe and Ni nanoparticles on graphene,[15,16] and (v) unzipping of carbon nanotubes by chemical oxidation.[17,18] However, it is still a challenging task to produce nanosized graphene with atomically well-defined edges. This is partially due to the difficulty in controlling the cutting direction of the graphene

(1) Novoselov, K. S.; Geim, A. K.; Morozov, S. V.; Jiang, D.; Katsnelson, M. I.; Grigorieva, I. V.; Dubonos, S. V.; Firsov, A. A. *Nature* **2005**, *438*, 197–200.
(2) Novoselov, K. S.; Jiang, Z.; Zhang, Y.; Morozov, S. V.; Stormer, H. L.; Zeitler, U.; Maan, J. C.; Boebinger, G. S.; Kim, P.; Geim, A. K. *Science* **2007**, *315*, 1379.
(3) Geim, A. K.; Novoselov, K. S. *Nat. Mater.* **2007**, *6*, 183–191.
(4) Fujita, M.; Wakabayashi, K.; Nakada, K.; Kusakabe, K. *J. Phys. Soc., Jpn.* **1996**, *65*, 1920–1923.
(5) Nakada, K.; Fujita, M.; Dresselhaus, G.; Dresselhaus, M. S. *Phys. Rev. B* **1996**, *54*, 17954–17961.
(6) Kobayashi, Y.; Fukui, K.; Enoki, T.; Kusakabe, K.; Kaburagi, Y. *Phys. Rev. B* **2005**, *71*, 193406.
(7) Kobayashi, Y.; Fukui, K.; Enoki, T.; Kusakabe, K. *Phys. Rev. B* **2006**, *73*, 125415.
(8) Fernández-Rossier, J.; Palacios, J. J. *Phys. Rev. Lett.* **2007**, *99*, 177204.
(9) Wang, W. L.; Meng, S.; Kaxiras, E. *Nano Lett.* **2008**, *8*, 241–245.
(10) Wu, J.; Pisula, W.; Müllen, K. *Chem. Rev.* **2007**, *107*, 718–747.
(11) Chen, Z.; Lin, Y.-M.; Rooks, M. J.; Avouris, P. *Phys. E* **2007**, *40*, 228–232.
(12) Han, M. Y.; Ozyilmaz, B.; Zhang, Y.; Kim, P. *Phys. Rev. Lett.* **2007**, *98*, 206805.
(13) Li, X.; Wang, X.; Zhang, L.; Lee, S.; Dai, H. *Science* **2008**, *319*, 1229–1232.
(14) Tapasztó, L.; Dobrik, G.; Lambin, P.; Biró, L. P. *Nat. Nanotechnol.* **2008**, *3*, 397–401.
(15) Datta, S. S.; Strachan, D. R.; Khamis, S. M.; Johnson, A. T. C. *Nano Lett.* **2008**, *8*, 1912–1915.
(16) Ci, L.; Xu, Z.; Wang, L.; Gao, W.; Ding, F.; Kelly, K. F.; Yakobson, B. I.; Ajayan, P. M. *Nano Res.* **2008**, *1*, 116–122.
(17) Kosynkin, D. V.; Higginbotham, A. L.; Sinitskii, A.; Lomeda, J. R.; Dimiev, A.; Price, B. K.; Tour, J. M. *Nature* **2009**, *458*, 872–877.
(18) Jiao, L.; Zhang, L.; Wang, X.; Diankov, G.; Dai, H. *Nature* **2009**, *458*, 877–880.

10.1021/ja101265r

sheet during rather destructive fabrication processes such as the lithographic and chemical etching.

Here we show a simple approach to produce nanographene[19] with a well-defined edge by cutting up a preoxidized graphene sheet in a less destructive manner using a noncontact atomic force microscopic (NC-AFM) manipulation technique.[20] Oxidized sheets with linear defects that could result from the ordered linear arrangement of oxygen-containing functional groups[21−28] are selected for the cutting experiments. The linear defect acts as a chemical template to direct the edge cutting during and after NC-AFM manipulation, and thus the resulting edges should have well-defined shape originating from the ordered atomic structure in the line defect. In the following, we will first present the structural and electronic characterization of oxidized graphene sheets used in this study by means of NC-AFM imaging and spectroscopy under ultrahigh vacuum (UHV) conditions (sections 3.1 and 3.2). We then focus on detailed structural analysis of the linear defects in the oxidized sheets and correlate them with the ordered arrangement of oxygen functional groups with assistance from an extensive set of recent theoretical predictions[21−28] (section 3.3). Finally, we demonstrate how oxidized sheets with linear defects can be cut into nanosized pieces (section 3.4).

2. Experimental Section

The oxidized graphene samples studied here were prepared from natural graphite (Kanto Chemical and Kojundo Chemical Laboratory) by the conventional Hummer's method[29] using $KMnO_4$ and H_2SO_4. In a typical reaction, 1 g of graphite and 50 mL of H_2SO_4 were stirred together in an ice bath, and then 6 g of $KMnO_4$ was slowly added. Once mixed, the solution was stirred for approximately 1 h, forming a thick paste. An amount of 50 mL of water was then added, and the solution was stirred for 30 min while the temperature was raised to 30 °C. Finally, 100 mL of water was added, followed by the slow addition of 6 mL of H_2O_2 (30%). The solution was then filtered, and the oxidized samples were purified by washing with 10% HCl solution and repeated rinsing with deionized water (Millipore, Milli Q water). After drying in an oven at 80 °C for 24 h, the purified samples were redispersed in deionized water and exfoliated into single layers by mechanical agitation in an ultrasonic bath. To remove large aggregates of unexfoliated layers, the dispersed solution was centrifuged at 1000 rpm for 5 min. The supernatant was drop-cast onto freshly cleaved highly oriented pyrolytic graphite (HOPG) substrates or SiO_2/Si substrates. After 30 min, the excess solvent was removed, and the substrate was transferred into the UHV chamber for AFM measurements.

All AFM measurements were performed in UHV (ca. 5×10^{-8} Pa) at room temperature. A commercially available AFM system (VT beam-deflection AFM, Omicron) with a phase-locked-loop unit (Easy PLL-plus, Nanosurf) for frequency modulation feedback[20] was used. NC-AFM images were acquired using a silicon cantilever (NSC11, MikroMasch) or a platinum-coated silicon cantilever (NSC11/Ti−Pt). The cantilevers were oscillated with a constant peak-to-peak amplitude of ca. 20 nm at their resonant frequency. The resonant frequency and force constant of the cantilevers were 350−450 kHz and 40−50 N/m, respectively.

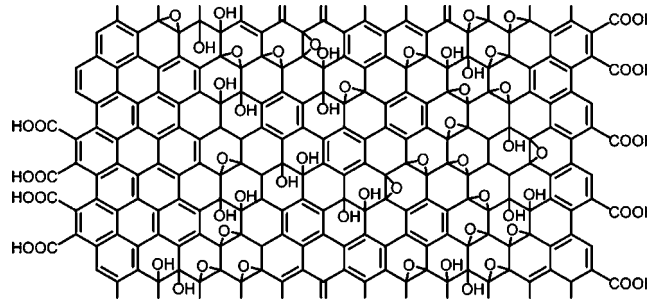

Figure 1. Structural model of graphite oxide proposed by Lerf et al. (modified and adapted from ref 33).

3. Results and Discussion

3.1. Surface Morphology on the Oxidized Graphene Sheets. Oxidized graphite, graphite oxide (GO), has been known for over 100 years,[30] but its structure has not yet been precisely determined.[31] There is extensive nuclear magnetic resonance, infrared spectroscopic, and electron diffraction evidence for the presence of COOH, OH, and C═O groups at the edge of the graphene sheet, while the basal plane is covered with mostly epoxide and OH groups;[31−34] however, variable stoichiometry and the local arrangement of oxygen-containing functional groups is unclear and is still a matter of discussion.[31] Oxidized graphene is usually derived from the exfoliation of GO and is therefore likely to share a similar structure. According to recently proposed models, OH, epoxide, and a small amount of C═O groups are randomly distributed over the top and bottom of a graphene sheet.[31−33] The most well-known structural model, proposed by Lerf et al.,[33] is depicted in Figure 1.

Figures 2(a) and (b) show NC-AFM topographic images of oxidized graphene sheets on atomically smooth HOPG substrates. In both images, corrugated sheets with a lateral size of ca. 200×200 nm^2 are evident. It should be noted here that in a separate experiment oxidized graphene sheets were deposited on atomically rough SiO_2/Si substrates that are technologically relevant to electronic device fabrication and have been used in most of the previous studies; however, the contribution of the substrate roughness to the observed topography of the graphene sheets was not negligible. Recent studies have shown that graphene sheets strongly follow the corrugations of the underlying substrates.[35−38] In our AFM study, it was very difficult to

(19) Enoki, T.; Takai, K. *Solid State Commun.* **2009**, *149*, 1144–1150.
(20) Morita, S.; Wiesendanger, R.; Meyer, E. *Noncontact Atomic Force Microscopy*; Springer: Berlin, 2002.
(21) Li, J.-L.; Kudin, K. N.; McAllister, M. J.; Prud'homme, M. J.; Aksay, I. A.; Car, R. *Phys. Rev. Lett.* **2006**, *96*, 176101.
(22) Schniepp, H. C.; Li, J.-L.; McAllister, M. J.; Sai, H.; Herrera-Alonso, M.; Adamson, D. H.; Prud'homme, R. K.; Car, R.; Saville, D. A.; Aksay, I. A. *J. Phys. Chem. B* **2006**, *110*, 8535.
(23) Kudin, K. N.; Ozbas, B.; Schniepp, H. C.; Prud'homme, R. K.; Aksay, I. A.; Car, R. *Nano Lett.* **2008**, *8*, 36–41.
(24) Gao, X.; Wang, L.; Ohtsuka, Y.; Jiang, D.; Zhao, Y.; Nagase, S.; Chen, Z. *J. Am. Chem. Soc.* **2009**, *131*, 9663–9669.
(25) Li, Z.; Zhang, W.; Luo, Y.; Yang, J.; Hou, J. G. *J. Am. Chem. Soc.* **2009**, *131*, 6320–6321.
(26) Kutana, A.; Giapis, K. P. *J. Phys. Chem. C* **2009**, *113*, 14721–14726.
(27) Yan, J.-A.; Xian, L.; Chou, M. Y. *Phys. Rev. Lett.* **2009**, *103*, 086802.
(28) Xu, Z.; Xue, K. *Nanotechnology* **2010**, *21*, 045704.
(29) Hummers, W. S.; Offeman, R. E. *J. Am. Chem. Soc.* **1958**, *80*, 1339.
(30) Brodie, B. C. *Philos. Trans. R. Soc.* **1859**, *149*, 249–259.
(31) Dreyer, D. R.; Park, S.; Bielawski, C. W.; Ruoff, R. S. *Chem. Soc. Rev.* **2010**, *39*, 228–240.
(32) Szabó, T.; Berkesi, O.; Forgó, P.; Josepovits, K.; Sanakis, Y.; Petridis, D.; Dékány, I. *Chem. Mater.* **2006**, *18*, 2740–2749.
(33) Lerf, A.; He, H.; Forster, M.; Klinowski, J. *J. Phys. Chem. B* **1998**, *102*, 4477–4481.
(34) Aragon de la Cruz, F.; Cowley, J. M. *Nature* **1962**, *196*, 468–469.
(35) Ishigami, M.; Chen, J. H.; Cullen, W. G.; Fuhrer, M. S.; Williams, E. D. *Nano Lett.* **2007**, *7*, 1643–1648.
(36) Stolyarova, E.; Rim, K. T.; Ryu, S.; Maultzsch, J.; Kim, P.; Brus, L. E.; Heinz, T. F.; Hybertsen, M. S.; Flynn, G. W. *Proc. Natl. Acad. Sci. U.S.A.* **2007**, *104*, 9209–9212.
(37) Stöberl, U.; Wurstbauer, U.; Wegscheider, W.; Weiss, D.; Eroms, J. *Appl. Phys. Lett.* **2008**, *93*, 051906.
(38) Lui, C. H.; Liu, L; Mak, K. F.; Flynn, G. W.; Heinz, T. F. *Nature* **2009**, *462*, 339–341.

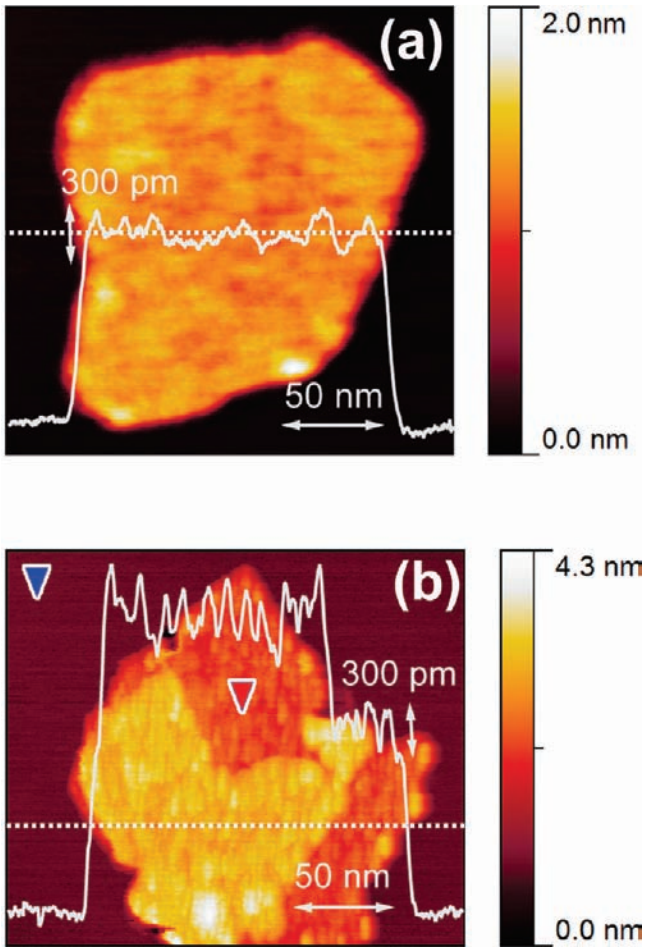

Figure 2. NC-AFM image of oxidized graphene sheet with a height profile (z-scale bar = 300 pm) taken along the dotted line. Imaging conditions: (a) cantilever = NSC11/Pt, frequency shift (Δf) = −10 Hz, sample bias voltage (V_b) = 0 V; (b) cantilever = NSC11/Pt, Δf = −15 Hz, V_b = +0.1 V.

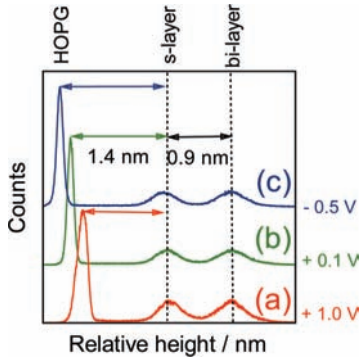

Figure 3. Height histograms obtained from NC-AFM images of the oxidized sheet (Figure 2(b)) taken at three different sample bias voltages of (a) +1.0, (b) +0.1, and (c) −0.5 V. The NC-AFM images taken at (a) V_b = +1 V and (c) −0.5 V are not shown.

evaluate intrinsic corrugations of the oxidized sheets on SiO_2 substrates. Therefore, the AFM characterization presented in this paper was performed using atomically smooth HOPG substrates.

Figure 3 shows histograms of heights over the bilayer and single-layer regions in the sheet and the HOPG substrate obtained from NC-AFM images acquired at three different sample bias voltages (V_b = +1.0, +0.1, and −0.5 V). One of

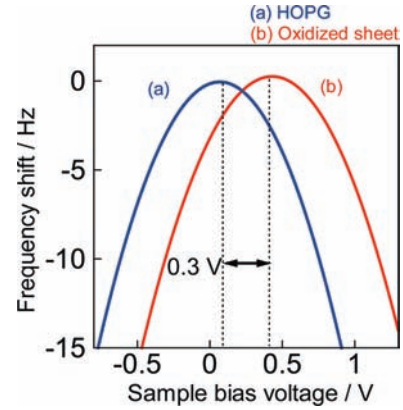

Figure 4. Frequency shift (electrostatic force) versus sample bias voltage curves measured for the oxidized single sheet (red arrow in Figure 2(b)) and HOPG substrate (blue arrow in Figure 2(b)).

the images is shown in Figure 2(b) (V_b = +0.1 V). The histograms reveal that the apparent thickness of the single sheets is 1.2−1.5 nm, and the interlayer distance of the bilayer sheet is ca. 0.9 nm. The apparent topography measured by NC-AFM is subject to uncompensated residual electrostatic forces when the sample consists of regions with different local work functions (contact potential difference).[20,39,40] The difference in the local work functions of the sheet and the substrate can be estimated from force versus bias voltage measurements (Figure 4), in which the bias voltage to minimize the electrostatic force (i.e., frequency shift) on the single-layer region in the sheet is shifted positively by ca. 0.3 V relative to that on the substrate. A similar shift of +0.3 V was observed for the bilayer region using force versus bias voltage measurements (not shown here). When a sample bias voltage of +0.1 V was applied during the NC-AFM imaging (Figure 2(b)), the electrostatic force acting between the AFM tip and the sample is almost canceled out on the HOPG substrate, whereas additional uncompensated electrostatic force acts on the sheet (see Figure 4), which causes errors in the thickness measurement (i.e., the relative height measurement between the sheet and the substrate during constant force mode imaging[20]). The apparent thickness of the single-layer sheet was found to vary from 1.2 to 1.5 nm depending on the change in the uncompensated electrostatic force due to the bias voltage applied between the AFM tip and the substrate (in the range of V_b from −0.5 to +1.0 V), whereas the interlayer distance is independent of the bias voltage as can be seen in the height histograms of Figure 3. AFM has been routinely used to measure the thickness of pristine graphene and chemically functionalized graphene on several substrates; however, there is a large variation in the observed thicknesses of single sheets. The thickness ranges from 0.35 to 1.7 nm for graphene[41] and from 1.0 to 1.6 nm for oxidized graphene.[22,42−44] This variability

(39) Zerweck, U.; Loppacher, C.; Otto, T.; Grafström, S.; Eng, L. M. *Phys. Rev. B* **2004**, *71*, 125424.
(40) Sadewasser, S.; Carl, P.; Glatzel, T.; Lux-Steiner, M. C. *Nanotechnology* **2004**, *15*, S14–S18.
(41) Nemes-Incze, P.; Osvatha, Z.; Kamaras, Z.; Biro, L. P. *Carbon* **2008**, *46*, 1435–1442.
(42) Stankovich, S.; Dikin, D. A.; Dommett, G. H. B.; Kohlhaas, K. M.; Zimney, E. J.; Stach, E. A.; Piner, R. D.; Nguyen, S. T.; Ruoff, R. S. *Nature* **2006**, *442*, 282–286.
(43) Stankovich, S.; Dikin, D. A.; Piner, R. D.; Kohlhaas, K. A.; Kleinhammes, A.; Jia, Y.; Wu, Y.; Nguyen, S. T.; Ruoff, R. S. *Carbon* **2007**, *45*, 1558–1565.
(44) Li, D.; Müller, M.; Gilje, S.; Kaner, R. B.; Wallace, G. G. *Nat. Nanotechnol.* **2008**, *3*, 101–105.

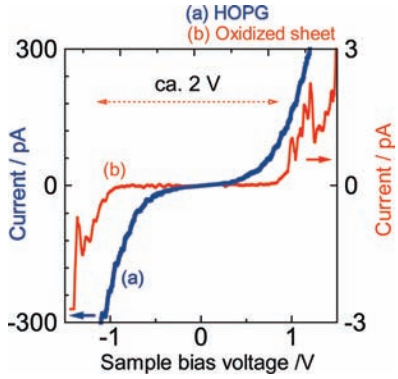

Figure 5. Current versus sample bias voltage curves measured for the oxidized single sheet (red arrow in Figure 2(b)) and HOPG substrate (blue arrow in Figure 2(b)).

could be partially due to the effect of the previously described uncompensated electrostatic forces. Scanning Kelvin probe microscopy[20] could be a useful method to cancel out the spatial variation in the uncompensated electrostatic forces to reduce errors in the film thickness measurement.

The sharp peaks for the HOPG substrate in Figure 3 indicate smooth surface morphology, while the broader peaks for the oxidized sheet can be ascribed to a corrugated structure, which can be interpreted as the result of modification of the original sp^2 carbon (C) atoms in graphene to sp^3 C atoms via bonding with oxygen (O)-containing functional groups.[31] That is, the bonding characteristics of the connecting C atoms change from planar sp^2 to distorted sp^3 hybridization with the new bonds formed between C and O atoms. In this process, C atoms are moved from their original positions to accommodate the off-plane tetrahedral sp^3 bonds. In Figure 2(a), the oxidized sheet displays a randomly corrugated structure, which implies inhomogeneous distribution of the oxygen-containing functional groups (epoxy and OH groups). The typical vertical variations are in the subnanometer range, and the lateral feature sizes are <10 nm. This result is in good agreement with the previous AFM study, where the surface morphology of oxidized graphene sheets was investigated in detail.[45] In contrast to the randomly corrugated structure, ordered wrinkles are apparent in Figure 2(b) with a width of ca. 10 nm that run a length of 10−50 nm along the *y*-axis in the image. The wrinkled structure is most likely due to the ordered local distribution of oxygen functional groups. A detailed discussion is presented in section 3.3.

3.2. Electronic Properties of Oxidized Graphene. The electronic properties of oxidized graphene have a strong correlation with the oxidation level;[46] therefore, the current versus sample-bias (I−V) characteristics were measured for the oxidized graphene sheet (Figure 2(b)). Figure 5 shows I−V characteristics measured for the HOPG substrate (blue curve) and the single-layered region in the oxidized sheet (red curve). Electrical conductivity measured on the oxidized sheet (i.e., tunneling current through the system composed of substrate/sheet/tip) displays a 2 orders of magnitude lower value than that on the HOPG substrate. The reduced electrical conductivity of the sheet can be explained by a decrease in the sp^2 carbon content in the sheet, in addition to ill-defined contacts between the corrugated sheet and the substrate (i.e., weak molecule−substrate interaction). The sudden increase in the tunneling current at a bias voltage of ±1 V implies that a band gap of ca. 2 eV is induced by oxidation. This is consistent with previous observations, in which graphite oxide samples displayed an optical band gap of 1.7−2.4 eV.[46] According to this result, the band gap of the graphite oxide samples is strongly correlated with the degree of oxidation (i.e., atomic ratio of O/C). The band gap of ca. 2 eV observed in our study corresponds to an oxidation level with an atomic ratio of O/C = 0.20−0.25.[46] It should be noted that this ratio is comparable to that of the model (O/C = 0.22) in Figure 1.

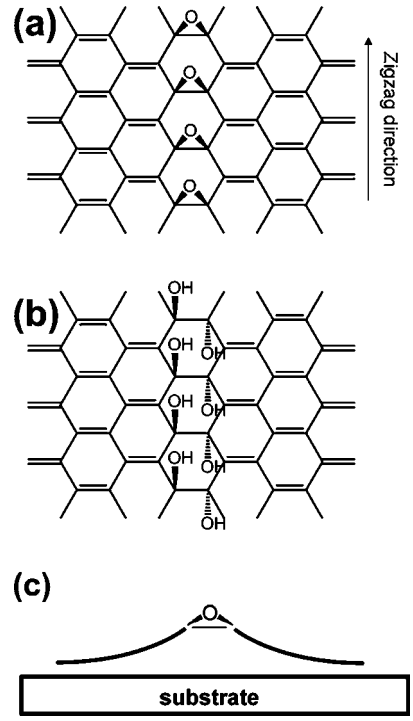

Figure 6. Possible ordered arrangement of the (a) epoxide and (b) OH groups on a graphene sheet. (c) Side view of model (a) on a substrate (modified and adapted from refs 26 and 28).

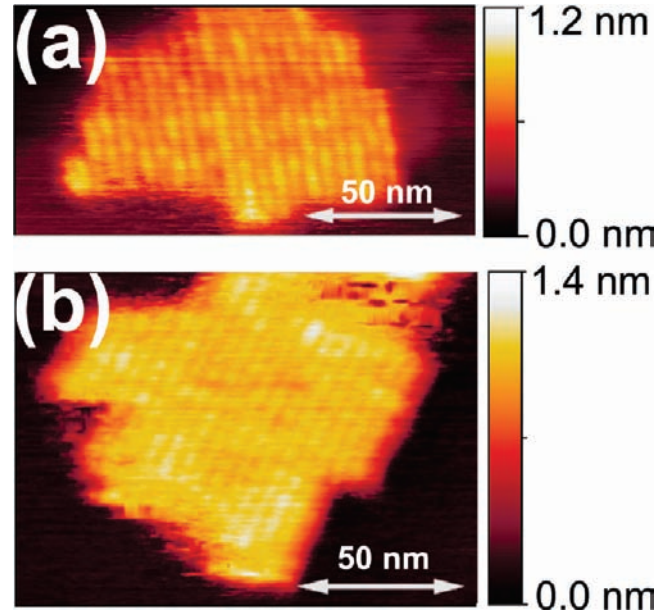

Figure 7. NC-AFM images of the oxidized single graphene sheets with ordered wrinkles. Imaging conditions: cantilever = NSC11, $\Delta f = -10$ Hz, $V_b = +0.5$ V.

(45) Paredes, J. I.; Villar-Rodil, S.; Fernández,., P. S.; Alonso, A. M.; Tascón, J. M. D. *Langmuir* **2009**, *25*, 5957–5968.
(46) Jeong, H. K.; Jin, M. H.; So, K. P.; Lim, S. C.; Lee, Y. H. *J. Phys. D: Appl. Phys.* **2009**, *42*, 065418.

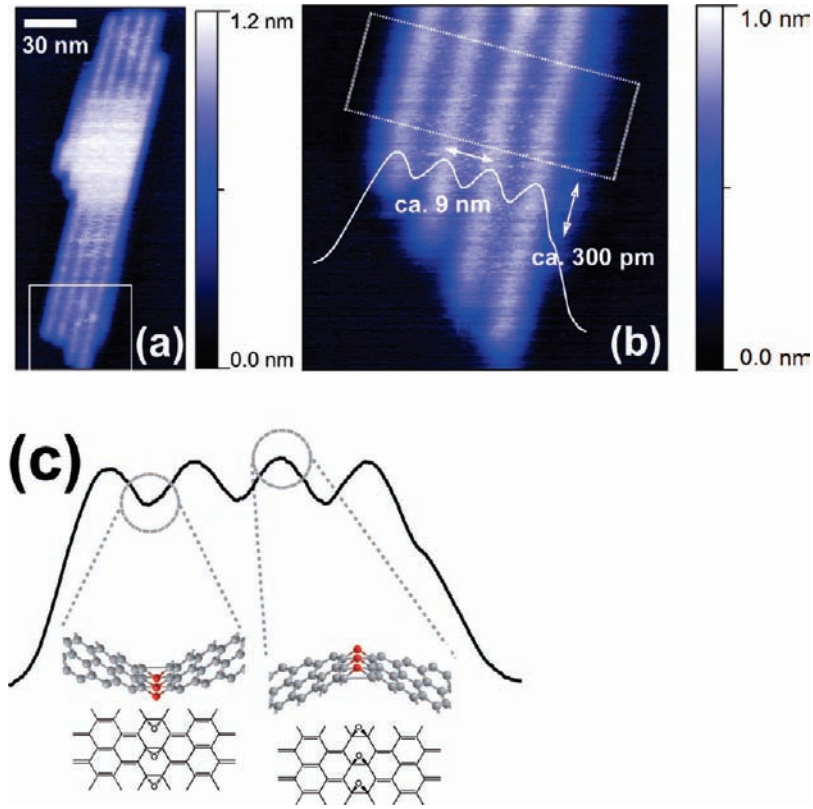

Figure 8. (a) NC-AFM image of the oxidized single graphene sheet with ordered wrinkles. (b) Magnified NC-AFM image of the area indicated by the white square in (a). Averaged height profile obtained for the dotted area indicated in (b) is superimposed on the image (z-scale bar = 300 pm). Imaging conditions: cantilever = NSC11, $\Delta f = -20$ Hz, $V_b = 0$ V. (c) Possible structural model of the linear epoxy groups for the observed height profile in (b) is shown. In the stick and ball model, carbon and oxygen atoms are colored gray and red, respectively.

3.3. Ordered Arrangement of Oxygen Functional Groups. Although most of the recent studies on local structural characterization of oxidized graphene sheets have indicated large structural disorder in the carbon skeleton due to a random arrangement of oxygen functional groups[22,31,45,47,48] (Figure 1), there have been some experimental reports[49−52] and theoretical predictions[21−28] that suggest an ordered carbon skeleton originating from the ordered local arrangement of oxygen-containing functional groups. We note here that it has been known for over 40 years, from X-ray diffraction studies, that layered graphene oxide sheets (i.e., graphite oxide) retain strong crystalline order.[34] Recent high-resolution transmission electron microscopic imaging of a single graphene oxide sheet showed a clear graphitic lattice distributed over the range of >10 nm,[48] and Raman spectroscopy measurements suggested an ordered structure of ribbon-like graphitic lattice (graphitic ribbon-like domains) surrounded by oxidized regions to explain the Raman shift in graphite oxide.[52] However, direct observation of ordered local oxidized structures has been limited to a few previous studies.[49,50]

Following the two models proposed by Kudin et al.[52] and Li et al.,[21] the ordered arrangement of epoxide and OH groups on graphene sheets are depicted in Figures 6(a) and (b), respectively. The epoxide and OH groups were suggested to have a preference for linear alignment.[21−28,50,52] In particular, the linear arrangement of epoxide groups causes higher angular strain in the epoxide rings that could bend the sheet as shown schematically in Figure 6(c). Such a bent structure has been predicted in several theoretical studies[21−28] and could be responsible for the wrinkles observed in Figure 2(b). Figures 7, 8(a), and 10(a) show NC-AFM topographic images of other oxidized single sheets that exhibit similar, but clearer, wrinkles. The coexistence of the ordered structure of the wrinkles with the disordered one (Figure 2(a)) can be interpreted as the result of strong oxidation process, in which intercalates of the sulfuric acid (bisulfate) molecules and oxidative agents[53] are inhomogeneously inserted between the graphene layers. Such inhomogeneous distribution, that is, domain structure of intercalates, has been proposed for graphite intercalation compounds.[54,55] There could be local variations in oxidized structures of the graphene sheets depending on the differences in the local oxidative environment due to the inhomogenesous distribution of the intercalates. The

(47) Mkhoyan, K. A.; Contryman, A. W.; Silcox, J.; Stewart, D. A.; Eda, G.; Mattevi, C.; Miller, S.; Chhowalla, M. *Nano Lett.* **2009**, *9*, 1058–1063.
(48) Wilson, N. R.; Pandey, A.; Beanland, R.; Young, R. J.; Kinloch, I. A.; Gong, L.; Liu, Z.; Suenaga, K.; Rourke, J. P.; York, S. J.; Sloan, J. *ACS Nano* **2009**, *3*, 2547–2556.
(49) Phaner-Goutorbe, M.; Sartre, A.; Porte, L. *Microsc. Microanal. Microstruct.* **1994**, *5*, 283–290.
(50) Pandey, D.; Reifenberger, R.; Piner, R. *Surf. Sci.* **2008**, *602*, 1607–1613.
(51) Gomez-Navarro, C.; Weitz, R. T.; Bittner, A.; Scolari, M.; Mews, A.; Burghard, M.; Kern, K. *Nano Lett.* **2007**, *7*, 3499–3503.
(52) Kudin, K. N.; Ozbas, B.; Schniepp, H. C.; Prudhomme, R. K.; Aksay, I. A.; Car, R. *Nano Lett.* **2008**, *8*, 36–41.
(53) Sorokina, N. E.; Khaskov, M. A.; Avdeev, V. V.; Nikol'skaya, I. V. *Russ. J. Gen. Chem.* **2005**, *75*, 162–168.
(54) Hérold, A. *NATO ASI Ser. B* **1987**, *172*, 3–44.
(55) Enoki, T.; Suzuki, M.; Endo, M. *Graphite Intercalation Compounds and Applications*; Oxford University Press: New York, 2003.

exfoliated single sheets with disordered structure were often observed in our AFM images, and their size ranged from 100 to 2000 nm. The sheets with the ordered wrinkles were much less frequently found, and their size is 30−100 nm (Figures 7, 8(a), and 10(a)). Most of the oxidation of the graphene lattice proceeds in a rather random manner,[31] but there is presumably a local area where the ordered oxidation reaction occurs.

Detailed analyses of the corrugation in the ordered oxidized structure indicate that the wrinkle-ridges are regularly spaced with a width of 5−10 nm running a length of >100 nm along the ridges. Figure 8(b) shows an example of the cross sectional analysis, in which nearly periodic corrugation with a width of ca. 9 nm is apparent. The origin of the regular spacing of the ridges (i.e., periodicity of the oxidized structure) is unclear. According to recent research on nonoxidized graphene sheets, spontaneous formation of nearly periodic ripples (wrinkles) has been reported for suspended graphene sheets over trenches.[56] The origin of the periodic ripples can be adequately explained by classical theory of an elastic sheet, in which clumped boundary conditions imposed by banks of the trenches suppress lateral movement and induce local stress.[56] This behavior is one of the unique properties of graphene that is a flexible two-dimensional monatomic sheet. The high flexibility of the sheet could make it rather sensitive not only to the external forces (that originate from the clumped boundary conditions) but also to possible internal forces induced by chemical modification such as oxidation. We temporarily expect that the periodicity of the oxidized structure observed in our study is related to the spontaneous formation of the periodic ripples[56] during the oxidation process. Once the linear arrangement of the epoxide groups (Figure 6(a)) is formed, it induces the local stress in the sheet. The local stress could cause the periodic ripples, which could act as a template of subsequent formation of the linear arrangements of the epoxide groups on the ridges of the periodic ripples.

On the basis of the model in Figure 6(c), we propose a structural model for the observed wrinkles (Figure 8(c)). Here we assume that the linear epoxide groups are present on the top and bottom of the sheet because both sides are accessible to oxidizing agents during the oxidation reaction. The linear arrangement of the epoxide groups induces large strain in the epoxy rings and can lead to the breaking of C−C bonds in a concerted fashion. This has been proposed for the oxidation-induced unzipping mechanisms of graphitic materials, such as carbon nanotubes[14] and graphene.[21] However, it is still not clear how the graphene sheet can eventually break up because even after the rupture of C−C bonds the graphene sheets remains interconnected by O atoms. A very recent theoretical study predicts that the bonding between the two C atoms in the highly strained epoxide ring is almost balanced out by the ring strain.[26] Consequently, additional perturbation of the rings is necessary for the rupture of the C−C bond and/or C−O bond in the ring. To confirm the theoretical prediction and provide evidence for our hypothesis that the observed wrinkles are caused by highly strained linear epoxy groups, we tested whether the wrinkled region could be ruptured by application of mechanical stress, and this is presented in the following section.

3.4. Cutting the Oxidized Graphene Sheets. A point contact was made between the wrinkled sheet and the AFM probe to apply local mechanical stress. The detailed procedure of the AFM manipulation is described in ref 57. Figure 9 shows a series of NC-AFM images of the oxidized single sheet with ordered wrinkles (a) before and (b)−(f) after the contact process. The point contact is made several times at the center of the sheet (Figure 9(a)), which leads to a cut-out of the wrinkled nanodomains around the contact region (Figure 9(b)). There are two types of cut edge shape: one is linear along the ridge of the wrinkle as expected (thick straight red lines in Figure 9(a)), and the other has a curved feature (thin curved red lines in Figure 9(a)). Details of the two types of cut edge shape are discussed in the following paragraph. After the nanodomains have been cut out, the sheet starts to spontaneously break up with cut edges similar to those shown in Figure 9(b). This self-breaking process occurs in an uncontrollable manner, and the sheet is divided into two pieces (Figure 9(f)). It is interesting to note that the oxidized sheet in Figure 9 displays elastic response[56] to the AFM manipulation. The middle part of the oxidized sheet initially

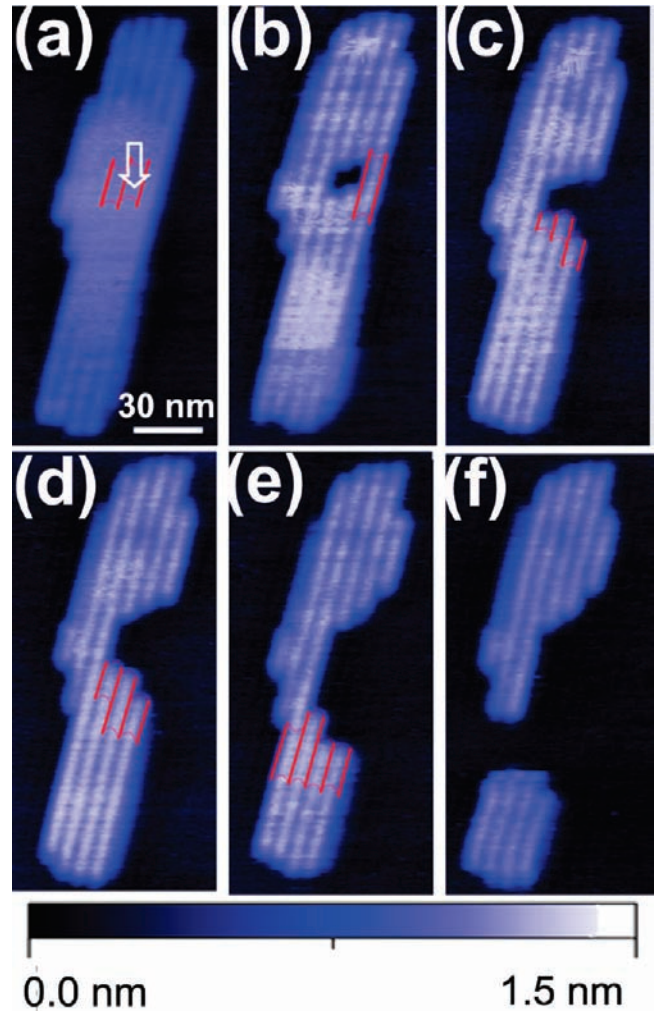

Figure 9. Series of NC-AFM images of the oxidized sheet with ordered wrinkles during and after the AFM manipulation experiment. Images were acquired at time intervals of ca. 5−10 min. (a) The point contact between the sheet and the AFM probe is made at the center of the sheet. The contact area is indicated by a white arrow. The region indicated by the red line is cut out during the point contact experiment. (b−f) The sheet then starts to spontaneously break up with segmentations of the regions indicated by the red lines. Imaging conditions: cantilever = NSC11, $\Delta f = -40-50$ Hz, $V_b = 0$ V.

(56) Bao, W.; Miao, F.; Chen, Z.; Zhang, H.; Jang, W.; Dames, C.; Lau, C. N. *Nat. Nanotechnol.* **2009**, *4*, 562–566.

(57) (a) Fujii, S.; Fujihira, M. *Jpn. J. Appl. Phys.* **2006**, *45*, 1986–1991. (b) Fujii, S.; Fujihira, M. *Nanotechnology* **2006**, *17*, S112–S120.

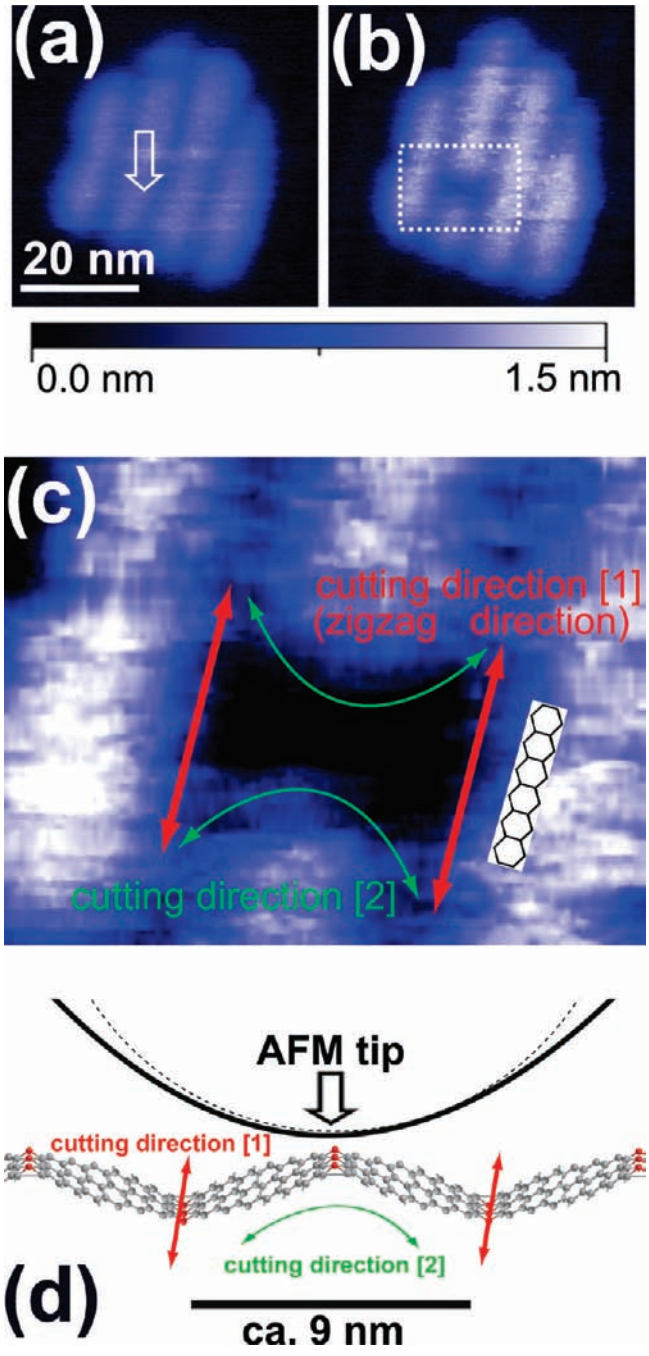

Figure 10. (a),(b) NC-AFM images of the oxidized sheet with the ordered wrinkles (a) before and (b) after the AFM manipulation experiment. The point contact was made on the region indicated by the white arrow in (a). (c) Magnified NC-AFM image of the dotted area in (b). Two distinct types of cutting direction of [1] and [2] are indicated by red and green arrows, respectively. The direction [1] is along the ridges, and thus the resulting edge is expected to be terminated by the zigzag edge structure as schematically illustrated on the image. Imaging conditions: cantilever = NSC11, $\Delta f = -30$ Hz, $V_b = 0$ V. (d) Schematic illustration of the cut-out event. The point contact between the wrinkle (see also the models in Figures 6(a) and 8(c)) and AFM tip with a nominal radius of 10 nm causes cutting out of the nanodomain along the two distinct types of direction [1] and [2].

displays flat surface (Figure 9(a)), but a clear wrinkled structure appears after the nanodomains have been cut out (Figure 9(b)). Strain, possibly due to the imperfect periodicity of the oxidized structure with respect to the graphene lattice, is likely to be relaxed after the nanodomains have been cut out. This observation could be experimental evidence that the observed sheet is not self-assembled nanostructure which is constructed from residual impurities from the solvent. This observation could be experimental evidence that the observed sheet is the oxidized graphene sheet which exhibits the elastic property of thin films.

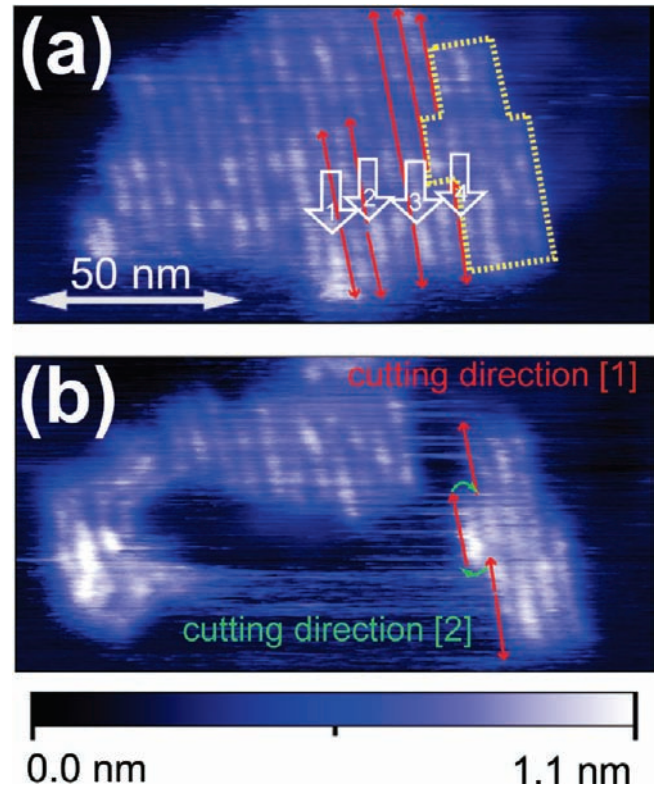

Figure 11. (a),(b) NC-AFM images of the oxidized sheet with the ordered wrinkles (a) before and (b) after the AFM manipulation experiment. This sheet is the same as that shown in Figure 7(a). The point contact was made several times on the regions indicated by the white arrows in (a), which lead to rupture of the sheet along the ridges as indicated by red arrows, and a sheet outlined by dotted lines is cut out. In (b), the two types of cutting direction of [1] and [2] are reproducibly observed. Imaging conditions: cantilever = NSC11, $\Delta f = -10$ Hz, $V_b = +0.5$ V.

To obtain further insight into the two types of edge shape, another point contact experiment was conducted with another oxidized sheet having ordered wrinkles (Figures 10(a) and (b)), where the cutting out of the wrinkled nanodomain was reproducibly observed. Figure 10(c) shows a magnified image of the cut edges, where two distinct types of cutting direction are again observed. These are, respectively, indicated by linear arrows (i.e., cutting direction [1]) and curved arrows (cutting direction [2]) in Figure 10(c). On the basis of the structural models shown in Figures 6(a) and 8(c), schematic illustration of the cut-out event is shown in Figure 10(d). The linear edge shape along the ridge of the wrinkle is consistent with our expectation as described in the previous chapter and can thus be attributed to the result of breakage along the linear epoxide groups, while the curved edge shape could be caused by the absence of order in the oxidized structure along the cutting direction. We were unable to obtain the edge resolution required to confirm this, so this remains to be clarified in future study.

Without knowing the exact cut edge structure, we demonstrate how a relatively large sheet with the ordered wrinkles is cut into small pieces with the well-defined edge. Figure 11 shows NC-AFM images of the oxidized sheet before and after the point contact process. We tried to prepare a small sheet with a width

similar to those shown in Figures 8(a) and 10(a). After the several point contact experiments, the sheet with the width of 30−40 nm is prepared as indicated by dotted lines in Figure 11(a). In this cutting experiment, approximately 80% of the cut edges show desired shape along the ridges (i.e., zigzag direction) as indicated by the red straight arrows in Figure 11(b). For the remaining 20% of cut edges indicated by green curved arrows,[58] the cut edge structure is not well-defined, and it is unclear which type of edge (i.e., zigzag or armchair edge) is predominant. We should note here that a bottom-up approach of chemical synthesis of nanographene has reported preferred formation of nanographene molecules with armchair edges,[10] and integration of zigzag edges into molecules has been limited to a few cases.[59]

Successful cutting experiments of oxidized sheets were achieved only for the oxidized sheets with the ordered wrinkles. In the three cutting experiments presented above, approximately 50−80% of the cut edges show the desired shape along the ridges (see the flakes (i) in the upper part of Figure 9(f), (ii) in Figure 10(b), and (iii) in the right side of Figure 11(b)). Cutting of the randomly corrugated sheet was hardly observable. Repeated point contact experiments eventually led to more failure in an uncontrollable manner than rupture of the sheets. A similar tendency has been recently reported for lateral AFM manipulation of thermally reduced graphene oxide sheets,[60] in which lateral movement and folding of the sheets, instead of rupture, have been observed during the manipulation experiments. Previous studies on cutting of nonoxidized graphene sheets by AFM manipulation technique[61,62] also suggest difficulty in controlling cutting direction, which is mostly due to high flexibility[63] of the graphene sheets. For the control of the cutting direction, the ordered oxidized structure (i.e., the linear arrangement of the epoxide groups) could play an important role.

(58) The percentage was roughly calculated from the total edge-length for the two types of the cut edge (e.g., see the length of the red and green arrows in Figure 11(b)).

(59) Wang, Z.; Tomović, Ž.; Kastler, M.; Pretsch, R.; Negri, F.; Enkelmann, V.; Müllen, K. *J. Am. Chem. Soc.* **2004**, *126*, 7794–7795.

4. Conclusions

The structural and electronic properties of oxidized graphene sheets were characterized using NC-AFM imaging and SPM spectroscopy under UHV conditions at room temperature. An ordered local arrangement of oxygen-containing functional groups was observed on the sheet, which is likely to be a linear arrangement of epoxide groups. The linear arrangement bends the sheet in a concerted manner, which appears in the AFM images as a wrinkle with a width of 5−10 nm and a length of >100 nm. This interpretation is in part supported by recent theoretical calculations. NC-AFM manipulation experiments performed on the wrinkles show the wrinkled nanodomains are cut out of the sheet and have a well-defined cut edge along the ridge (i.e., the linear epoxide groups), and the cut is most likely to be aligned with the zigzag direction of the graphene lattice in the sheet. This cutting procedure of the graphene sheet could be a useful method for the production of nanographene with well-defined edges.

Acknowledgment. This work was supported by a Grant-in-Aid for Specially Promoted Research No. 20001006 from the Ministry of Education, Culture, Sports, Science and Technology (MEXT), Japan.

JA101265R

(60) Schniepp, H. C.; Kudin, K. N.; Li, J.-L.; Prud'homme, R. K.; Car, R.; Saville, D. A.; Aksay, I. A. *ACS Nano* **2008**, *2*, 2577–2584.

(61) Giesbers, A. J. M.; Zeitler, U.; Neubeckb, S.; Freitag, F.; Novoselov, K. S.; Maan, J. C. *Solid State Commun.* **2008**, *147*, 366–369.

(62) Eliers, S.; Rabe, J. P. *Phys. Status Solidi B* **2009**, *246*, 2527–2529.

(63) Lee, C.; Wei, X.; Kysar, J. W.; Hone, J. *Science* **2008**, *321*, 385–388.